

Body-size scaling in an SEI model of wildlife diseases

Luca Bolzoni^{a,*}, Giulio A. De Leo^a, Marino Gatto^b, Andrew P. Dobson^c

^a *Dipartimento di Scienze Ambientali, Università degli Studi di Parma, Parco Area delle Scienze 11/A, 43100 Parma, Italy*

^b *Dipartimento di Elettronica e Informazione, Politecnico di Milano, Via Ponzio 34/5, 20133 Milano, Italy*

^c *Department of Ecology and Evolutionary Biology, Princeton University, Princeton, NJ 08544-1003, United States*

Received 16 January 2007

Available online 31 January 2008

Abstract

A number of wildlife pathogens are generalist and can affect different host species characterized by a wide range of body sizes. In this work we analyze the role of allometric scaling of host vital and epidemiological rates in a Susceptible-Exposed-Infected (SEI) model. Our analysis shows that the transmission coefficient threshold for the disease to establish in the population scales allometrically (exponent = 0.45) with host size as well as the threshold at which limit cycles occur. In contrast, the threshold of the basic reproduction number for sustained oscillations to occur is independent of the host size and is always greater than 5. In the case of rabies, we show that the oscillation periods predicted by the model match those observed in the field for a wide range of host sizes.

The population dynamics of the SEI model is also analyzed in the case of pathogens affecting multiple coexisting hosts with different body sizes. Our analyses show that the basic reproduction number for limit cycles to occur depends on the ratio between host sizes, that the oscillation period in a multihost community is set by the smaller species dynamics, and that intermediate interspecific disease transmission can stabilize the epidemic occurrence in wildlife communities.

© 2007 Elsevier Inc. All rights reserved.

Keywords: Allometry; SEI model; Wildlife diseases; Bifurcation analysis; Multihost

1. Introduction

Pathogens are a ubiquitous, often neglected component of biodiversity which may have a tremendous impact on the population dynamics of their hosts and can play an important role in shaping the structure of ecological communities. Some pathogens, such as rabbit haemorrhagic disease virus, are species-specific, others, such as rabies or distemper viruses, are quite generalist and can affect many different host species. Of the many traits characterizing host species demography, body size is probably the most influential one, as many demographic parameters scale allometrically with host body size (Peters, 1983; Calder, 1984). Larger hosts are thus expected to have longer life expectancy, smaller reproductive rate, slower dynamics and more sparse populations densities when

compared to smaller host species. Such scaling laws imply that ecological systems complexity can be reduced by considering processes according to their inherent scale. This approach has been used to describe food web structure (Cohen et al., 2003), home-range area (Jetz et al., 2005), and pathogens spread (De Leo and Dobson, 1996).

In the case of generalist pathogens, it is interesting to investigate how threshold conditions for the disease to invade and establish in a parasite-free host population change with different body size. Of course, many different ecological and epidemiological factors – ranging from immune response to interspecific competition, animal behavior, feeding habits etc. – can regulate the ability of a pathogen to successfully establish in a host population. Some basic epidemiological parameters, such as the life expectancy of infected individuals and the time from inoculation to the first symptom, may exhibit a quite regular scaling pattern over a wide range of host species that may all be potentially infected by the same pathogen. For instance, in a recent study, Cable and Enquist (unpublished manuscript) have used epidemiological data on 16 host species

* Corresponding author.

E-mail addresses: luca.bolzoni@nemo.unipr.it (L. Bolzoni), giulio.deleo@unipr.it (G.A. De Leo), gatto@elet.polimi.it (M. Gatto), dobber@Princeton.EDU (A.P. Dobson).

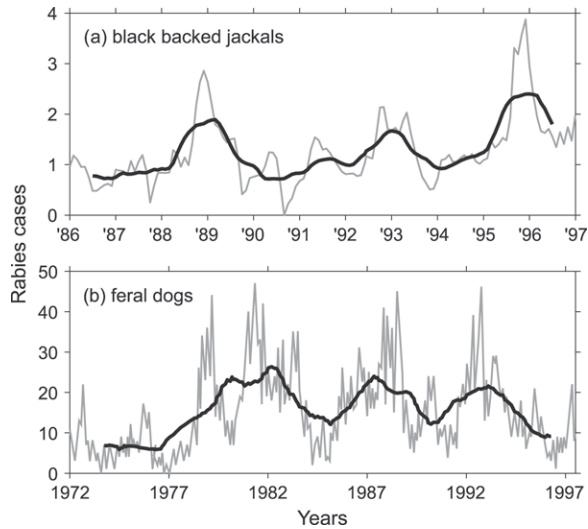


Fig. 1. Rabies confirmed cases (gray lines) with (a) moving 12-month centered mean (b) and 24-month centered mean (black lines) among black-backed jackals in central Namibia, 1986–1996 (a, data from Courtin et al. (2000)) and feral dogs in Santa Cruz, Bolivia, 1972–1997 (b, data from Widdowson et al. (2002)). Time series show sustained oscillations in the total number of infected in different host populations.

affected by pseudorabies virus (PRV, *Herpesvirus suis*), 11 species by anthrax (*Bacillus anthracis*), and 21 species by rabies (*Lyssavirus sp.*) to show that interspecific variations in the host metabolic rate, which highly correlates to body size, strongly influence the timing of pathogenesis. As a consequence, epidemiological parameters such as the length of the latent period and the disease-induced mortality may also scale allometrically with host body size. Based on the evidence of allometric scaling available at the time, (De Leo and Dobson, 1996), without inferring relationships between transmission and size, had used a simple Susceptible-Infected (SI) model to show that transmission coefficients necessary to produce comparable values of R_0 in different species are themselves allometric functions of host body size. Here, we use a similar approach for an SEI (Susceptibles, Exposed, Infected) model of rabies that takes into account the empirical finding by Cable and Enquist (unpublished manuscript). We extend the pioneering model by Anderson et al. (1981), who were first in proposing an SEI approach to study rabies in the wildlife, by explicitly accounting for the influence of body size. The dynamics of the SEI model can be more complex than the one predicted with a simpler SI (and SIR) model: in particular, if the latent period (the average time spent in the exposed class) is sufficiently long, the population dynamics of the infected host can be characterized by sustained oscillations (Swart, 1989; Pugliese, 1991). Epidemic cycles of this kind have already been observed in the field for many species infected by rabies, such as black-backed jackals (Courtin et al., 2000; Walton and Joly, 2003) and feral dogs (Bingham et al., 1999; Widdowson et al., 2002). See examples in Fig. 1.

In the present paper we explore how disease invasion and epidemic occurrence can depend on the host metabolic rates and body size. To address these issues, we first recast the basic

Anderson et al. (1981) SEI model setting the birth and death rates and the carrying capacity of the host population as simple allometric functions of host body size. In accordance with the analysis of Cable and Enquist (unpublished manuscript) the latent period and the disease-induced mortality rate are also assumed to scale allometrically with host body size. Threshold conditions are analyzed under different assumptions on disease mortality and on the time spent in the exposed class by the hosts.

Recent work showed that single-host/single-pathogen relationships are not able to capture the epidemic dynamics in wildlife communities, because generalist pathogens may cause ‘apparent competition’ between hosts (Hudson and Greenman, 2002) and cross-species transmission can modify pathogen evolution (Woolhouse et al., 2001). To account for this important point we extend a previous work by Dobson (2004) on a multiple-host SI model of wildlife disease and analyze the population dynamics of an SEI model in the case of interspecific transmission among hosts with different body size. Interspecific infections pose dramatic problems in conservation biology as shown by the case of Serengeti National Park where the lion population (*Panthera leo*) has been endangered by the canine distemper virus epidemic in feral dogs (*C. lupus familiaris*) (Cleaveland et al., 2000), and Ethiopian wolves (*Canis simensis*) and African wild dogs (*Lycaon pictus*) have been threatened by rabies epidemics in feral dogs (Gascoyne et al., 1993; Sillero-Zubiri et al., 1997). Moreover, multihost models can be used to explain other epidemic dynamics, for example when host populations are not able to support infection endemically without reintroduction from outside species sources (‘disease spillover’ and ‘apparent multihost’ according to the classification of Fenton and Pedersen (2005)). In the case of rabies there are a lot of similar examples, such as gray wolf (*C. lupus*) epidemics supported by foxes in North America (Brand et al., 1995) and side-striped jackal (*Canis adustus*) epidemics supported by dogs in Zimbabwe (Rhodes et al., 1998). Specifically, we want to identify the conditions under which a reservoir host species can drive other host species to extinction and analyze the population dynamics of multiple interacting hosts characterized by different body sizes.

The paper is organized as follows: in the next section we present the basic structure of the allometric SEI model. In the third and fourth section, threshold conditions and model bifurcation diagrams are derived analytically and numerically with reference to the most important epidemiological parameters (latent period and disease mortality) and over a wide range of possible host body sizes. In the fifth section, we analyze the population dynamics of two host species characterized by different body size when a pathogen can affect both species with some degree of interspecific transmission. The results are finally summarized and discussed in the concluding section. Although specific numerical analyses have been developed by taking rabies as the reference disease, the structure of the model analyzed in the present work is quite general and can be considered valid for a range of lethal diseases of the wildlife. Therefore, the implications of our findings are quite broad.

2. The allometric SEI model

The epidemiology of a lethal disease within a homogeneous wildlife population has been traditionally modeled by partitioning the host population into three epidemiological classes – Susceptible (S), Exposed (E , i.e., infected but not yet infectious) and Infective (I) individuals – and by describing population dynamics of the three classes by means of ordinary differential equations. This simple deterministic approach was first developed in the seminal work of Anderson et al. (1981) to predict the impact of rabies in the European fox. We develop our analysis using the same model because, despite the simplicity of its formulation, it has been able to grasp the main features of observed epidemiological trends. In its original version, the SEI model assumes logistic growth of the host species in the absence of rabies, density-dependent transmission of the disease, and reproduction of disease-free animals only. Recovery and immunity are not included in the basic model. The ordinary differential equations that describe the dynamics of densities in the three population classes are:

$$\frac{dS}{dt} = \nu S - (\mu + \gamma N)S - \beta SI \quad (1a)$$

$$\frac{dE}{dt} = \beta SI - (\sigma + \mu + \gamma N)E \quad (1b)$$

$$\frac{dI}{dt} = \sigma E - (\alpha + \mu + \gamma N)I \quad (1c)$$

where $N = S + E + I$ is the total population density, ν and μ are the intrinsic birth and death rates, γ is the intraspecific competition coefficient (with $\gamma = r/K$, where $r = \nu - \mu$ is the intrinsic growth rate and K the carrying capacity), β is the transmission coefficient, σ is the rate at which an infected individual becomes infective ($1/\sigma$ being the mean latency period of rabies) and α the disease-induced mortality. By summing the right-hand sides of the Eqs. (1), one obtains the dynamics of N , namely:

$$\frac{dN}{dt} = \nu S - (\mu + \gamma N)N - \alpha I. \quad (1d)$$

In order to account for a variety of mammalian host species, one can assume, as evidenced by Peters (1983), Silva and Downing (1995) and De Leo and Dobson (1996), that the basic vital rates scale allometrically with the host body size w as follows:

$$\begin{aligned} \nu &= w^{-0.25} \\ \mu &= 0.4w^{-0.25} \\ K &= 16.2w^{-0.70} \end{aligned} \quad (2)$$

where w is expressed in kilograms, ν , μ and r in year⁻¹ and K in individuals/km². Cable and Enquist (unpublished manuscript) have also shown that the basic epidemiological parameters scale allometrically with the host body size in the same way as μ . Accordingly, we have assumed that the latent period ($1/\sigma$) and the infectious period ($1/\alpha$) – representing respectively the average time spent in the exposed and the infective class – are proportional to the mean life expectancy

of the disease-free host ($1/\mu$) at low population density. More precisely, we assume that:

$$\begin{aligned} \sigma &= n\mu = n0.4w^{-0.25} \\ \alpha &= m\mu = m0.4w^{-0.25} \end{aligned} \quad (3)$$

where n and m are always greater than one, because the times spent in exposed and infective classes are shorter than the mean life expectancy. For example, in the case of rabies in foxes, the host life expectancy is about 2 years, while the incubation period is one month and the life expectancy after infection is only a few days (about 5). Obviously, large values of the two parameters n and m correspond to pathogens with short latency period and high disease mortality rate, respectively. Integrating the relationships (2) and (3) into the original Anderson et al. (1981) system (1) produces a body-size-dependent model for rabies or diseases with similar characteristics. Contrary to σ and α , there is no evidence that the transmission coefficient β scales allometrically with host body size. Moreover, the transmission coefficient measurements are often difficult as it can be estimated only from extensive field data (Begon et al., 1999). For this reason, in the next section we will perform a sensitivity analysis of model (1) behaviors for a broad range of β values.

3. Stability analysis and thresholds

Before exploring the influence of host body size w on the population dynamics of the host–pathogen relationship, it is important to briefly review the main features of model (1) which has been thoroughly analyzed elsewhere (Swart, 1989). For convenience we consider model (1) in the variables N , E , I using Eqs. (1b)–(1d) in which we set $S = N - E - I$. The model (1) has three equilibrium points: the trivial equilibrium $X_0 = (0, 0, 0)$, the disease-free equilibrium $X_1 = (K, 0, 0)$, and the enzootic equilibrium $X_2 = (N_{eq}, E_{eq}, I_{eq})$, where:

$$\begin{aligned} N_{eq} &= (\nu\xi + \nu + \alpha)(\beta - \phi\nu)^{-1} \\ I_{eq} &= (r - \gamma N_{eq})\beta^{-1} \\ E_{eq} &= (\xi + \phi N_{eq})I_{eq} \end{aligned}$$

with $\xi = (\alpha + \mu)/\sigma$ and $\phi = \gamma/\sigma$.

The equilibrium X_2 is biologically meaningful only when $N_{eq}, E_{eq}, I_{eq} \geq 0$.

By analyzing the eigenvalues of the Jacobian matrix of model (1) it is possible to determine the stability of the three equilibria (see Swart (1989) for details). The trivial equilibrium point X_0 represents the extinction of the host species and is always unstable when $\nu > \mu$. The disease-free equilibrium X_1 , at which the host population is at its carrying capacity in absence of the disease, is stable if and only if

$$R_0 = \frac{\sigma\beta K}{(\sigma + \nu)(\alpha + \nu)} = 6.48\beta \frac{n}{(0.4n + 1)} \frac{w^{-0.45}}{(0.4m + 1)} < 1 \quad (4)$$

where the parameter R_0 is the basic reproduction number of the disease, that is the expected number of secondary cases produced by an infected host introduced into a susceptible

population at its carrying capacity (Anderson and May, 1991). Thus, the basic reproduction number scales allometrically with body size via the exponent -0.45 as in the SI model (De Leo and Dobson, 1996). Moreover, R_0 decreases with increasing disease mortality (which grows with m), while it increases and levels off with decreasing latent period (namely, with increasing n). In particular, R_0 tends to zero with decreasing n , because no epidemic can establish with an infinite latency period, while R_0 increases with n up to an asymptotic value which corresponds to a vanishing latency period (as in the SI model by De Leo and Dobson (1996)). It is easy to prove that the enzootic equilibrium X_2 , representing the case in which rabies persists endemically in the host population, becomes epidemiologically feasible (that is strictly positive) when X_1 loses its stability, i.e., as soon as R_0 exceeds unity. The manifold in the parameter space defined by equation $R_0 = 1$ is thus characterized by a transcritical bifurcation (Kuznetsov, 1995) in which the two equilibrium points X_1 and X_2 collide and exchange their stability.

The condition for X_2 to be positive can also be expressed as

$$\beta > \beta_{TC} = \frac{(\sigma + \nu)(\alpha + \nu)}{\sigma K} = (0.4m + 1) \frac{(0.4n + 1)}{6.48n} w^{0.45}. \quad (5)$$

Therefore, we can state that the disease can persist in the host population if and only if the transmission coefficient of the disease β is above a minimum threshold value (called β_{TC}). The threshold for the transmission coefficient (β_{TC}) scales allometrically with body size (exponent $+0.45$), increases linearly with m and decreases with n down to an asymptotic minimum value, which corresponds to a vanishing latency period.

It can be shown analytically that the enzootic equilibrium X_2 undergoes a supercritical Hopf bifurcation with the emergence of limit cycles when R_0 is sufficiently high, more precisely when

$$\beta > \beta_H = 0.037 \frac{w^{0.45}}{\Gamma_0(n, m)} \quad (6)$$

where $\Gamma_0(n, m)$, function of n and m only, represents the smaller positive solution of equation number 6 in Swart (1989, p. 201) when one replaces the model parameters with expressions (2) and (3) (see Appendix A for details). In simpler words, for $\beta < \beta_H$ the enzootic equilibrium X_2 is stable, while for $\beta > \beta_H$ there are stable sustained oscillations. From an epidemiological viewpoint, the reason for oscillations was explained by Anderson et al. (1981): rabies acts as a time-delayed density-dependent regulator of wildlife population growth, the time lag being determined by how long the host population density remains below a critical size. This will largely be influenced by host birth rates. The transmission coefficient along the Hopf bifurcation (β_H) scales allometrically with exponent $+0.45$, just as the value β_{TC} did along the transcritical bifurcation.

A particularly interesting result is derived by looking at how the basic reproduction number R_0 changes along the Hopf bifurcation manifold. By substituting expression (6) for β_H into (4), it is easy to prove that the value of the basic reproduction

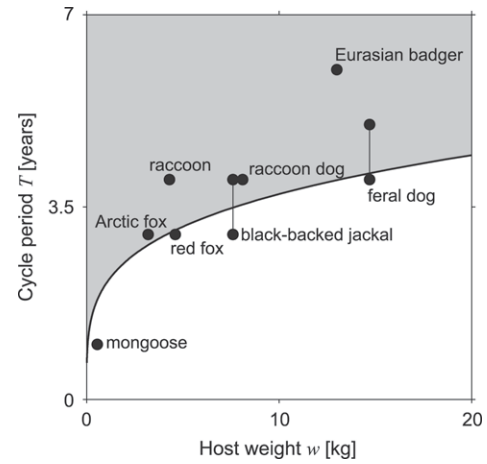


Fig. 2. The relationship between host body size and the period of sustained oscillations. The thick black line represents the period of cycles arising along the Hopf bifurcation, while the gray area represents feasible periods of sustained oscillations as predicted by the SEI model. The black points represent the minimum epizootic cycle period observed in the field for a range of mammal species affected by rabies. Thin lines connect points related to the same species. Data for: yellow mongoose (*Herpestes javanicus*), Arctic fox (*Alopex lagopus*), northern raccoon (*Procyon lotor*), red fox (*Vulpes vulpes*), black-backed jackal (*Canis mesomelas*), raccoon dog (*Nyctreutes procyonides*), Eurasia badger (*Meles meles*), and feral dog (*Canis familiaris*). See Supplementary Material for data details.

number along the Hopf bifurcation manifold does not depend on the body size w of the host species but is a function of the epidemiological parameters n and m only. However, the period of the epizootic cycle corresponding to the Hopf bifurcation does grow with the host body size w . In fact, along the Hopf bifurcation the oscillation period T (in years) of the densities in the three compartments of the host population is:

$$T = \frac{2\pi}{\rho} \quad (7)$$

where $\rho = \sqrt{\gamma N_{eq}(\alpha + \sigma + 2\mu + 2\gamma N_{eq})}$ is the modulus of the imaginary eigenvalues at the bifurcating enzootic equilibrium. By replacing Eqs. (2) and (3) into (7), it can be proved that T grows allometrically with body size with exponent $+0.25$.

Despite the simplicity of the mathematical formulation, the model is able to qualitatively grasp the dynamical behavior of wildlife diseases observed in nature for which it is known that host species with larger body size exhibit a larger period of epizootic cycles. As illustrated in Fig. 2, the expected duration of the oscillation period derived by our model matches quite well with that observed in the field for a number of different wildlife species affected by rabies (black dots). In Fig. 2 the solid line represents the minimum oscillation period of epidemics predicted by the SEI model (i.e., the period of cycles originating at the Hopf bifurcation), while the gray area shows feasible cycle periods for each host body size.

To sum up, the SEI model behavior is completely determined by body size w , transmission coefficient β , latency rate n and disease mortality m . The complete bifurcation diagrams in the w - β , n - β , and m - β spaces are easily derived from Eqs. (5) and (6). These curves are shown in Fig. 3: in each

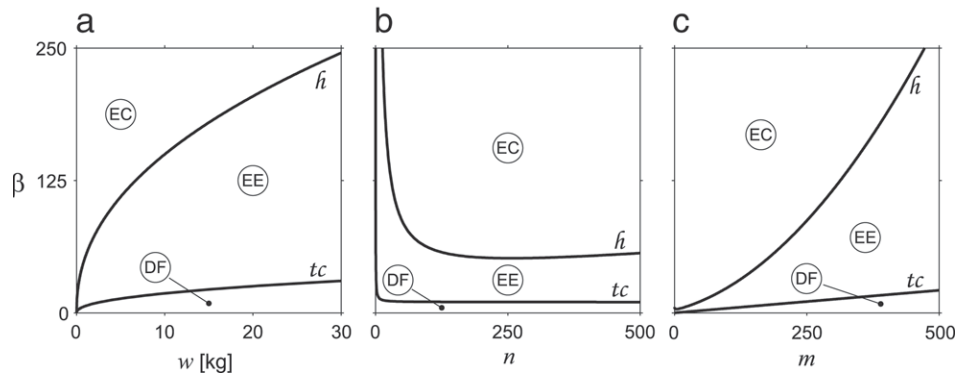


Fig. 3. Bifurcation diagrams of the SEI model in the w - β space (a), n - β space (b), and m - β space (c). In region DF (disease-free equilibrium) the virus becomes extinct. In region EE (enzootic equilibrium) the parasite survives in a constant host population. In region EC (epizootic cycle) the parasite survives in a fluctuating host population. The curve tc marks transcritical bifurcations and the curve h marks Hopf bifurcations. Other parameters set to: $m = 250$, in (a) and (b), $n = 50$, in (a) and (c), and $w = 3$ kg, in (b) and (c).

of the three bifurcation diagrams a transcritical bifurcation curve (tc) separates a region DF , where the disease-free equilibrium is the only attractor of the model (1), from a region EE , where the model variables are attracted to the enzootic equilibrium. Through a supercritical Hopf bifurcation curve (h) the system enters the region EC : here the enzootic equilibrium is unstable and an attracting epizootic periodic solution appears, whose period increases with host body size w . Fig. 3(a) shows the bifurcation diagram in the w - β space. In the previous section we showed that the transmission coefficient (β) scales allometrically with host body size with exponent $+0.45$ along both the transcritical and the Hopf bifurcation curves (see Eqs. (5) and (6)). Fig. 3(b), which shows the bifurcation diagram in the n - β space, demonstrates that the Hopf bifurcation curve exhibits a minimum when $n = m$, namely when the duration of the latency period equals the average time to death of a diseased individual. Fig. 3(c) shows the bifurcation diagram in the m - β space: the transcritical bifurcation curve is a linear function of m (see Eq. (5)); the Hopf bifurcation curve has a barely visible minimum for m equal to unity (i.e., natural mortality equals disease-induced mortality), but of course realistic values of m are much larger than one, as we explained above.

We showed that, along the Hopf bifurcation, R_0 is a function of the epidemiological parameters n and m only, not of host body size. How R_0 value changes along the Hopf bifurcation for different values of these parameters is reported in Fig. 4. It shows that limit cycles arise only for large values of the basic reproduction number. On the other hand, even for high values of R_0 , limit cycles occur only for intermediate n or m . In fact, if the latent period is very short, the SEI model tends to the SI model, while if it is too long, it tends to an SE model, neither of which can exhibit limit cycles (Gao et al., 1995; De Leo and Dobson, 1996). Interestingly enough, Fig. 4 shows that the Hopf bifurcation curves present a minimum R_0 when $n = m$, exactly as β_H does in Fig. 3(b). This is true regardless of the specific value of n and m , as long as the duration of the latency period equals the expected time to death of a diseased individual. We can hypothesize a sort of resonance effect, in which similar average times spent in E and I classes favor the

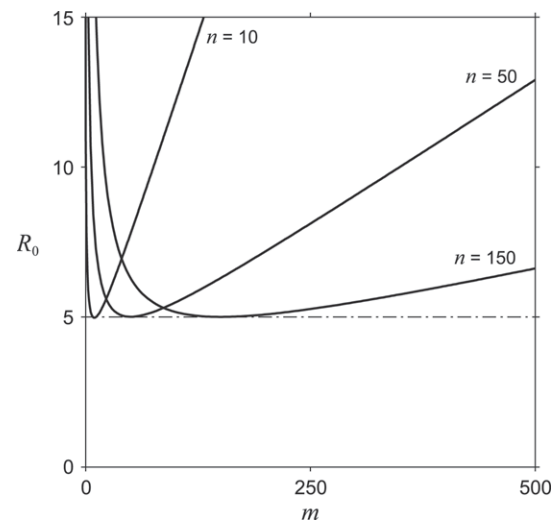


Fig. 4. Hopf bifurcation curves of the SEI model, computed by varying m and β (as in Fig. 3(c)), plotted in the m - R_0 space for different values of the relative latency rate n . Unspecified parameter values as in Fig. 3(c).

onset of oscillations. Moreover, the minimum value of R_0 for limit cycles to occur is about 5, regardless of host body size and specific values assigned to the allometric functions (2). In addition, we numerically analyzed for fixed values of the basic reproduction number, the cycle period beyond the Hopf bifurcation (i.e., inside the regions EC of Fig. 3). It increases allometrically with host body size (with exponent $+0.25$) as along the Hopf bifurcation curve.

4. The multiple-host SEI model

As pathogens like rabies can affect and establish in a wide range of host species, there is a definite possibility that interspecific transmission may occur among hosts of different body sizes. In this section, we investigate the population dynamics of a multiple-hosts infection by extending the analysis performed by Dobson (2004) for a multihost SI model to an SEI model of two host species with interspecific

transmission, as described hereafter:

$$\begin{aligned} \frac{dS_i}{dt} &= v_i S_i - (\mu_i + \gamma_i N_i) S_i - S_i \sum_{j=1,2} \beta_{ij} I_j \\ \frac{dE_i}{dt} &= S_i \sum_{j=1,2} \beta_{ij} I_j - (\sigma_i + \mu_i + \gamma_i N_i) E_i \\ \frac{dI_i}{dt} &= \sigma_i E_i - (\alpha_i + \mu_i + \gamma_i N_i) I_i \end{aligned} \quad (8)$$

where $i, j = 1, 2$. As in Section 2, model parameters scale allometrically with the hosts' body size (Eqs. (2) and (3)). In addition, we assume that the disease has the same basic reproduction number in both populations. From now on, we assume that $w_1 < w_2$, without lack of generality. Then the intraspecific transmission coefficients β_{ii} (i.e., the transmission among individuals of the same species) can be obtained from Eq. (4) by using a unique value for R_0 and 2 different values for w . The interspecific transmission β_{ij} ($i \neq j$), which is the transmission among individuals of different species, is here assumed to be proportional to the mean of the intraspecific transmissions as in Dobson (2004), namely:

$$\beta_{ij} = c \left(\frac{\beta_{ii} + \beta_{jj}}{2} \right)$$

where $i, j = 1, 2$ and c is the strength of interactions between species. We have assumed that between-species transmission is more difficult than within-species transmission, so that $0 \leq c \leq 1$. Dobson (2004) has thoroughly discussed the threshold conditions for disease invasion in a multihost SI model. Here, besides invasion thresholds, we analyze conditions for which the populations exhibit epizootic cycles and conditions for which a host population acts as a disease reservoir and drives the other host to extinction. In particular, our analysis shows that model behaviors do not depend on the absolute value of the two species body sizes, but only on their ratio. Results are reported in Fig. 5 which shows the bifurcation diagrams of model (8) as a function of the degree of interspecific transmission c and the intraspecific basic reproduction number R_0 (assumed equal for both species) for different values of the ratio between the two species body sizes ($\delta w = w_2/w_1$). For this purpose we used a continuation method supported by the software LOCBIF (Khibnik et al., 1993) and CONTENT (Kuznetsov, 1998) which compute bifurcation curves starting from any bifurcation point by means of an adaptive prediction–correction continuation procedure with tangent prediction and Newton correction.

For low values of R_0 , at each level of interspecific transmission there exists only the disease-free equilibrium, in which the two species coexist in the absence of disease. Dashed curve tc_1^c in Fig. 5 represents transcritical bifurcations (infection threshold) between the disease-free equilibrium and the enzootic one, where the two species coexist and the disease is present with a constant prevalence. Owing to the operating interspecific transmission, there exist no equilibria corresponding to the disease being present in one species, not in the other one. So, the curve tc_1^c does not depend on δw , the ratio between the hosts' body sizes. As shown by Dobson (2004),

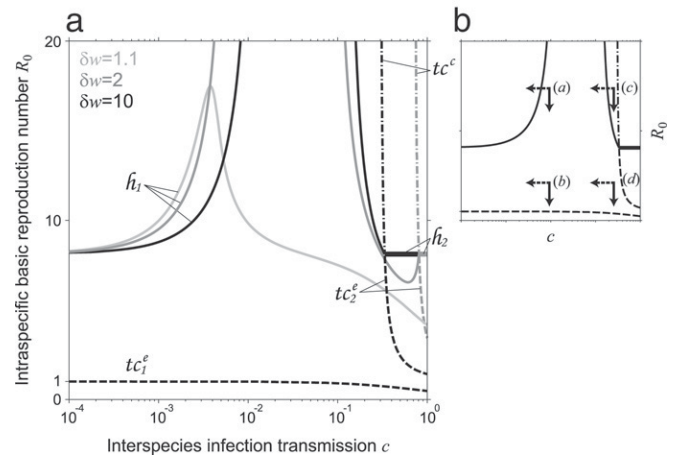


Fig. 5. Bifurcation diagram of the multiple-host SEI model (8) in the c – R_0 space (plotted in semi-logarithmic scale). (a) Two host species with different body-size ratio ($\delta w = w_2/w_1$): light gray curves ($\delta w = 1.1$), dark gray curves ($\delta w = 2$), and black curves ($\delta w = 10$). Thin solid lines (h_1), thick solid lines (h_2), dashed lines (tc_1^c), and dash-dotted lines (tc^c) represent the Hopf bifurcations of coexisting equilibria, Hopf bifurcations of one species equilibria, transcritical bifurcations of equilibria, and transcritical bifurcations of cycles (see text for details). Other parameters as in Fig. 3. (b) Arrows describe the effect of different control strategies in the case of $\delta w = 10$ and four different situations corresponding to low/high basic reproduction number and low/high interspecific infection transmission. Dotted arrows correspond to reduction of c (blocking tactics), solid arrows to reduction of R_0 (target and reservoir control). See discussion and conclusion paragraph for details.

when transmission is density-dependent as in model (8), the presence of more species of susceptible hosts implies that the number of contacts between infected individuals and potentially susceptible hosts increases. In fact, Fig. 5 shows that, for large level of interspecific transmission c , disease may invade host populations also for values of intraspecific basic reproduction number R_0 smaller than 1.

Solid curves (h_i) in Fig. 5 represent Hopf bifurcations: increasing values of R_0 lead stable enzootic equilibria to instability and give rise to stable epizootic cycles. Bifurcations h_1 involve attractors in which the two host population coexist, while bifurcations h_2 (which exist only for large values of δw) involve attractors in which the larger species is extinct. As a consequence, the value of the basic reproduction number at which bifurcations h_2 occur is independent of the value of interspecific transmission c .

By increasing δw a diseased host species that would exhibit sustained oscillations when isolated ($c = 0$) can be characterized by a stable infectious equilibrium when coexisting with another species with sufficiently different body size if interspecific transmission is intermediate (see solid curves in Fig. 5). A further (more detailed) analysis shows that the cycle period along Hopf bifurcations (h_i) is always close to that of the smaller species when isolated; therefore it is the smaller host species that drives the population dynamics setting the period of oscillations.

Curves tc_2^c represent transcritical bifurcations of coexistence equilibria: increasing values of interspecific transmission c or reproduction number R_0 drive the coexistence equilibrium to instability and the species with smaller body size outcompetes

the other which goes extinct. Similarly, curves tc^c represent transcritical bifurcations of limit cycles: increasing values of c destabilize the epizootic cycle at which the two host species coexisted and the host species with smaller body size outcompetes the other and keeps exhibiting sustained oscillations, according to the specific value of R_0 (as in model (1)). It is interesting to notice that curves tc_2^e and tc^c appear in the bifurcation diagram only for sufficiently high values of δw (dark gray and black curves in Fig. 5, which correspond to $\delta w = 2$ and $\delta w = 10$, respectively). This implies that high differences in size among host species may increase the extinction risk of the species with larger body size. Further analyses, not reported here, show similar pattern of behaviors for multiple-host model (8) with more than two host species ($i, j = 1, \dots, n$ with $n > 2$).

As remarked by Dobson (2004) for the SI model, a sufficiently high degree of interspecific transmission c can invariably drive to extinction the species with slower dynamics. Here, we have similar results, because the species that becomes extinct for sufficiently large c is the one with larger body size; this is also true when epizootic cycles occur.

5. Discussion and conclusions

In this work we have presented a class of simple SEI models in which basic vital rates and epidemiological parameters are set via allometric scaling with host body size in order to describe the spread of a lethal disease in a wide range of wildlife host species.

Our analysis shows that the minimum basic reproduction number R_0 necessary to sustain epizootic cycles does not depend upon host body size or allometric formulation of model parameters, but is a function of the relative duration of the latent period and the relative mean time to death of infected individuals with respect to the mean life expectancy of a disease-free host. The SEI model predicts that epizootic cycles cannot arise if the basic reproduction number is smaller than 5 regardless of host body size. This suggests the need of a sort of minimum activation energy (represented by the strength of R_0) for oscillation to arise, that is a structural property of the SEI model and not of the parameters chosen. On the other hand, field observations of rabid populations in the wild show that epizootic cycles may actually occur also for R_0 as low as 1.5–2.5 (Coleman and Dye, 1996; Kitala et al., 2002). As a consequence, it is possible that other factors, such as spatial dynamics or age structure or social hierarchy, and, most important, seasonal forcing, may actually play an important role in generating the observed patterns. The interplay between body size scaling of ecological and epidemiological parameters and these heterogeneity factors will be the subject of further investigations. Nevertheless, the relationship between host body size and the expected period of oscillations, as predicted by our SEI model, matches very well the field observations for a range of mammalian host species infected by rabies. Thus, our model might be used to roughly extrapolate the period of epizootic cycles in species for which data are not available.

Furthermore, simple extensions of the model are particularly suitable to describe infections in wildlife communities and networks consisting of animals with a spectrum of body sizes, in order to describe spillover, multiple-host, and multiple-pathogen dynamics. In the present work we have analyzed multiple-host interactions in the simple case of one pathogen infecting different host species. In the literature, several works analyzed parasite establishment (Holt et al., 2003; Dobson, 2004), host extinction risk (de Castro and Bolker, 2005; Fenton and Pedersen, 2005), and parasite evolution (Woolhouse et al., 2001; Gandon, 2004) in multihost communities, but little attention was paid to non-equilibrium behaviors. Here, we have put the stress on the epidemic events occurrence, deriving conditions for which epizootic cycles arise and underlining their features. We have found that, contrary to single-host models, the value of the basic reproduction number for sustained oscillation to occur strongly depends on the sizes of the two hosts (in particular on their ratio). Epidemic dynamics tends to stabilize for intermediate value of interspecific transmission c if species affected by the disease have different body sizes (see Fig. 5). Since c represents the level of coupling between population species, this result is in agreement with findings in metapopulation models of disease, in which intermediate level of host dispersal favors stability and synchrony of infections (Keeling and Rohani, 2002). Moreover, when two coexisting host populations exhibit limit cycles, the period of oscillation near the Hopf bifurcation is mainly driven by the smaller species. In addition, for sufficiently high values of interspecific transmission and species-size ratio, the host species with faster population dynamics (smaller body size) can drive the slower one (larger body size) to extinction. In practice, the smaller species acts as a disease reservoir. In fact, we have found that the extinction conditions of the larger species depend primarily on the transmission from the smaller host to the larger one (i.e., parameter β_{21} in model (8)). Therefore, policies for preventing the threatened host extinction should also devote efforts to avoiding reservoir–target transmission in addition to traditional measures such as vaccination of the endangered species.

There are other implications of our results for disease control in wildlife communities. Haydon et al. (2002) identified three different control strategies in multihost systems: *target control* and *reservoir control*, which are aimed at controlling infection within each populations (in model (8) the target is the larger size species and the reservoir is the smaller size one) and *blocking tactics*, to prevent transmission between species. These control strategies correspond to reducing R_0 and c in model (8), respectively. The benefits of these different approaches vary according to the difference in size of infected host species and to transmission conditions.

For host–pathogen systems with low interspecific transmission c , blocking tactics will be ineffectual, while control of within-species transmission proves to be effective under the same starting conditions. Indeed, in cases of high basic reproduction number (e.g., see point (a) in Fig. 5(b) in the case of large δw values), blocking tactics will drive the system toward large oscillations thus increasing the likelihood of host

stochastic extinction ‘during transient depression of population’ (sensu de Castro and Bolker, 2005), while target and reservoir controls tend to damp epizootic oscillations. In cases of low R_0 (see point (b) in Fig. 5(b)), control of within-species transmission is also more effective, driving the system toward the disease-free threshold.

On the contrary, for hosts–pathogen systems with high levels of c (points (c) and (d) in Fig. 5(b)), blocking tactics are effective because they move the target species away from extinction. Moreover, when R_0 is high (point (c) in Fig. 5(b)), they also reduce oscillation in the hosts’ populations. In cases of low R_0 (point (d) in Fig. 5(b)), control of within-species transmission is also effective, driving the system toward the disease-free threshold. In the light of these considerations, it turns out that an adequate estimation of transmission levels (within and between populations) is crucial to implementing effective control policies of rabies and similar diseases in wildlife systems.

The main features of the dynamics of the basic SEI body-size-dependent host–pathogen system are quite robust with respect to other variations in the model structure. In fact, further analysis not reported here demonstrates that results do not change substantially if we introduce spatial structure (patchy environment). Apparently, the introduction of more realistic details in the model does not significantly modify the relationship between the body size of the host and the characteristic transmission rate that allows for multi-years periodicity to occur. We suspect that allometry holds for a wide class of variations of the basic SEI models.

There are a large number of other diseases in which the host can develop temporary or permanent immunity. The introduction of an immunity class strongly changes the epidemic dynamics. Such model was analyzed by Coyne et al. (1989). They showed that even for small values of the immunity, the Hopf bifurcation that arises for increasing transmission rates in the SEI model disappears.

Recently, several works stressed the crucial role of social, spatial (Cross et al., 2005), and age/stage (Bolzoni et al., 2007) heterogeneity to understand transmission pattern of wildlife disease. In this context, the explicit introduction in the model of the host social organization will be an interesting development. For example, Brashares et al. (2000) show that group size in African antelope (family Bovidae) is allometrically related to species body size. This suggests that the within-group disease transmission in these species can be described as an allometric function of the body size as well.

Even though the relationships we found between host body size, transmission rate and resulting dynamics should not be interpreted as universal laws, they can provide useful hints on the kind of population dynamics in host–pathogen systems that is most likely to occur over a broad range of host body sizes. Information on the expected population dynamics can be used to design field campaigns to gather further data for the estimation of the basic epidemiological parameters. It is also useful to guide control and eradication policies, when action must be taken rapidly and information on host species is scanty, as it usually occurs in the case of many endangered populations.

Acknowledgments

The authors are indebted to Renato Casagrandi for his valuable and generous suggestions and remarks on a previous draft version of the manuscript. This work was supported by the National Center for Ecological Analysis and Synthesis (a Center funded by NSF no. DEB-0072909, the University of California at Santa Barbara, Seasonality and Infectious Diseases Group), the Italian Ministry of Research, the Istituto di Ingegneria Biomedica, CNR, Italy (M.G.), and the NIH/NSF Grant Number 128-4034 (A.P.D.).

Appendix A

The Hopf bifurcation condition for model (1) found by Swart (1989, Eq. (6) p. 201) is a 4th degree equation in the variable $\gamma\beta^{-1}$:

$$\begin{aligned}
 &(\gamma\beta^{-1})^4 v\alpha(Q + rv)^2 - (\gamma\beta^{-1})^3 \\
 &\quad \times [Q\{v(-v^2\alpha - v^2\sigma + 7\alpha v\sigma + v\alpha^2 + v\sigma^2 \\
 &\quad + v\mu\alpha + v\mu\sigma + 7\alpha^2\sigma + 7\alpha\sigma^2 - 2\alpha\sigma\mu) \\
 &\quad + 7\alpha^2\sigma^2\} + 4\sigma\alpha r^2 v^2] \\
 &\quad - (\gamma\beta^{-1})^2 \sigma [Q\{4\alpha^2 v + 4\sigma^2 v + 2\mu^2 v \\
 &\quad + 4\alpha\sigma v + 5\alpha\mu v + 2v^2\alpha + 2v^2\sigma - v^2\mu \\
 &\quad + 6\alpha^2\sigma + 6\alpha\sigma^2 + 13\alpha\sigma\mu\} - 6\alpha r^2\sigma v] \\
 &\quad - (\gamma\beta^{-1})\sigma^2 [Q\{\alpha^2 + \sigma^2 + 3\alpha\sigma + 6\alpha\mu + 6\sigma\mu + 2v\mu \\
 &\quad + 3\mu^2 - \alpha v + \sigma v\} + 4\alpha\sigma r^2] \\
 &\quad + \sigma^3 r [\mu(\alpha + \sigma + \mu) + \alpha\sigma] = 0 \tag{A.1}
 \end{aligned}$$

where $Q = v(\alpha + \sigma + \mu) + \alpha\sigma$.

By replacing allometric expressions (2) and (3) into Eq. (A.1), we obtain the following relationship:

$$\begin{aligned}
 &[(\gamma\beta^{-1})^4 \Gamma^4(n, m) + (\gamma\beta^{-1})^3 \Gamma^3(n, m) + (\gamma\beta^{-1})^2 \Gamma^2(n, m) \\
 &\quad + (\gamma\beta^{-1}) \Gamma^1(n, m) + \Gamma^0(n, m)] w^{-\frac{3}{2}} = 0 \tag{A.2}
 \end{aligned}$$

where the Γ^i 's ($i = 1, \dots, 5$) are suitable functions of n and m only. As shown by Swart (1989), Eq. (A.2) has two positive solutions, say $\Gamma_0(n, m)$ and $\Gamma_1(n, m)$, but only with the first (the smaller one) the inequality (5) – i.e., the existence of a positive endemic equilibrium – is satisfied. Hence, relationship (6) – i.e., $\beta = \gamma/\Gamma_0(n, m) = 0.037w^{0.45}/\Gamma_0(n, m)$ – guarantees the existence of two purely imaginary eigenvalues of the characteristic equation of model (1). Moreover, Swart (1989) has already proved that this solution satisfies the Hopf bifurcation transversality conditions. Then, relationship (6) represents the Hopf condition for model (1).

Appendix B. Supplementary material

Supplementary material associated with this article can be found, in the online version, at doi:10.1016/j.tpb.2007.12.003.

References

- Anderson, R., et al., 1981. Population dynamics of rabies in Europe. *Nature* 289, 765–771.
- Anderson, R., May, R., 1991. *Infectious Diseases in Humans: Dynamics and Control*. Oxford Science Publication, Oxford, UK.
- Begon, M., et al., 1999. Transmission dynamics of zoonotic pathogen within and between wildlife host species. *Proceedings of the Royal Society of London Series B* 266, 1939–1945.
- Bingham, J., et al., 1999. The epidemiology of rabies in Zimbabwe. 1. Rabies in dogs (*Canis familiaris*). *Onderstepoort Journal of Veterinary Research* 66 (1), 1–10.
- Bolzoni, L., et al., 2007. Transmission heterogeneity and control strategies for infectious disease emergence. *PLoS ONE* 2, e747.
- Brand, C., et al., 1995. Infectious and parasitic diseases of the gray wolf and their potential effects on wolf populations in North America. In Carbyn, L. (Ed.), *Ecology and Conservation of Wolves in a Changing World*. Canadian Circumpolar Institute, Edmonton, Canada, pp. 419–429.
- Brashares, J., et al., 2000. Phylogenetic analysis of coadaptation in behavior, diet, and body size in the African antelope. *Behavioral Ecology* 11, 452–463.
- Calder, W., 1984. *Size, Function, and Life History*. Dover Publications, Mineola, NY, USA.
- Cleaveland, S., et al., 2000. Serological and demographic evidence for domestic dogs as a source of canine distemper virus infection for Serengeti wildlife. *Veterinary Microbiology* 72 (3–4), 217–227.
- Cohen, J., et al., 2003. Ecological community description using the food webs, species abundance, and body size. *Proceedings of the National Academy of Sciences of the United States of America* 100, 1781–1786.
- Coleman, P., Dye, C., 1996. Immunization coverage required to prevent outbreaks of dog rabies. *Vaccine* 14 (3), 185–186.
- Courtin, F., et al., 2000. Temporal patterns of domestic and wildlife rabies in central Namibia stock-ranching area, 1986–1996. *Preventive Veterinary Medicine* 43, 13–28.
- Coyne, M., et al., 1989. Mathematical model for the population biology of rabies in raccoons in the mid-Atlantic states. *American Journal of Veterinary Research* 50, 2184–2154.
- Cross, P., et al., 2005. Duelling timescales of host movement and disease recovery determine invasion of disease in structured populations. *Ecology Letters* 8, 587–595.
- de Castro, F., Bolker, B., 2005. Mechanisms of disease-induced extinction. *Ecology Letters* 8, 117–126.
- De Leo, G., Dobson, A., 1996. Allometry and simple epidemic models for microparasites. *Nature* 379, 720–722.
- Dobson, A., 2004. Population dynamics of pathogens with multiple host species. *American Naturalist* 164 (5), S64–S78.
- Fenton, A., Pedersen, A., 2005. Community epidemiology framework for classifying disease threats. *Emerging Infectious Diseases* 11 (12), 1815–1821.
- Gandon, S., 2004. Evolution of multihost parasites. *Evolution* 58 (3), 455–469.
- Gao, L., et al., 1995. Four SEI endemic models with periodicity and separatrices. *Mathematical Biosciences* 128, 157–184.
- Gascoyne, S., et al., 1993. Aspects of rabies infection and control in the conservation of the African wild dog (*Lycaon pictus*) in the Serengeti region, Tanzania. *Onderstepoort Journal of Veterinary Research* 60, 415–420.
- Haydon, D., et al., 2002. Identifying reservoirs of infection: A conceptual and practical challenge. *Emerging Infectious Diseases* 8 (12), 1468–1473.
- Holt, R., et al., 2003. Parasite establishment in host communities. *Ecology Letters* 6, 837–842.
- Hudson, P., Greenman, J., 2002. Competition mediated by parasites: Biological and theoretical progress. *Trends in Ecology and Evolution* 13 (10), 387–390.
- Jetz, W., et al., 2005. The scaling of animal use space. *Science* 306, 266–268.
- Keeling, M., Rohani, P., 2002. Estimating spatial coupling in epidemiological systems: A mechanistic approach. *Ecology Letters* 5, 20–29.
- Khibnik, A., et al., 1993. Continuation techniques and interactive software for bifurcation analysis of ODEs and iterated maps. *Physica D* 62, 360–371.
- Kitala, P., et al., 2002. Comparison of vaccination strategies for control of dog rabies in Machakos District, Kenya. *Epidemiology and Infection* 129 (1), 215–222.
- Kuznetsov, Y., 1995. *Elements of Applied Bifurcation Theory*. Springer-Verlag, New York, NY, USA.
- Kuznetsov, Y., 1998. CONTENT — integrated environment for analysis of dynamical systems. Tutorial. Rapport de Recherche UPMA-98-224, Ecole Normale Supérieure de Lyon, Lyon, France.
- Peters, R., 1983. *The Ecological Implications of Body Size*. Cambridge University Press, Cambridge, UK.
- Pugliese, A., 1991. An SEI epidemic model with varying population size. In: Busenberg, S., Martelli, M. (Eds.), *Differential Equation Models in Biology, Epidemiology and Ecology*. In: *Lecture Notes in Biomathematics*, vol. 92. Springer-Verlag, New York, NY, USA, pp. 121–138.
- Rhodes, C., et al., 1998. Rabies in Zimbabwe: Reservoir dogs and the implications for disease control. *Philosophical Transactions of the Royal Society of London Series B* 353, 999–1010.
- Sillero-Zubiri, C., et al., 1997. *The Ethiopian Wolf — Status Survey and Conservation Action Plan*. IUCN, Gland, Switzerland.
- Silva, M., Downing, J., 1995. The allometric scaling of density and body mass: A nonlinear relationship for terrestrial mammals. *American Naturalist* 145, 707–727.
- Swart, J., 1989. Hopf bifurcation and stable limit cycle behavior in the spread of infectious diseases, with special application to fox rabies. *Mathematical Biosciences* 95, 199–207.
- Walton, L., Joly, D., 2003. *Canis mesomelas*. *Mammalian Species* 715, 1–9.
- Widdowson, M.-A., et al., 2002. Epidemiology of urban canine rabies, Santa Cruz, Bolivia, 1972–1997. *Epidemiology and Infection* 8, 458–461.
- Woolhouse, M., et al., 2001. Population biology of multihost pathogens. *Science* 292, 1109–1112.